



Design and Implementation of a Wideband Dual Polarized Plane Wave Generator with Tapered Feeding Non-Uniform Array

Zhang, Yusheng ; Wang, Zhengpeng ; Sun, Xuelei ; Qiao, Zhaolong ; Fan, Wei; Miao, Jungang

Published in:

I E E Antennas and Wireless Propagation Letters

DOI (link to publication from Publisher):

[10.1109/LAWP.2020.3010118](https://doi.org/10.1109/LAWP.2020.3010118)

Publication date:

2020

Document Version

Accepted author manuscript, peer reviewed version

[Link to publication from Aalborg University](#)

Citation for published version (APA):

Zhang, Y., Wang, Z., Sun, X., Qiao, Z., Fan, W., & Miao, J. (2020). Design and Implementation of a Wideband Dual Polarized Plane Wave Generator with Tapered Feeding Non-Uniform Array. *I E E Antennas and Wireless Propagation Letters*, 19(11), 1988-1992. Article 9143423. <https://doi.org/10.1109/LAWP.2020.3010118>

General rights

Copyright and moral rights for the publications made accessible in the public portal are retained by the authors and/or other copyright owners and it is a condition of accessing publications that users recognise and abide by the legal requirements associated with these rights.

- Users may download and print one copy of any publication from the public portal for the purpose of private study or research.
- You may not further distribute the material or use it for any profit-making activity or commercial gain
- You may freely distribute the URL identifying the publication in the public portal -

Take down policy

If you believe that this document breaches copyright please contact us at vbn@aub.aau.dk providing details, and we will remove access to the work immediately and investigate your claim.

Design and Implementation of a Wideband Dual Polarized Plane Wave Generator with Tapered Feeding Non-Uniform Array

Yusheng Zhang, Zhengpeng Wang, Xuelei Sun, Zhaolong Qiao, Wei Fan, Jungang Miao

Abstract—This paper presents a sub-6 GHz cost-effective wideband dual-polarized plane wave generator (PWG) design for 5G base station (BS) over-the-air (OTA) test. The proposed non-uniform PWG design is composed of 256 elements and has a dimension of 1.7 m×1.7 m. Several novel strategies are proposed and implemented to reduce the cost and complexity. To reduce feeding network complexity and mutual coupling among PWG elements, a novel tapered amplitude-only excitation method (i.e. with the same relative phase excitations among all PWG elements) is proposed. To reduce the number of channels in the phase and amplitude control network, a 4-element subarray is applied. Furthermore, wideband PWG element design and non-uniform configuration are applied to support for ultra-wideband operations from 2 GHz to 5 GHz. The proposed PWG design is numerically simulated and experimentally validated. A cylindrical quiet zone of a diameter of 0.9 m and a depth of 0.9 m, with 2.1 m distance to the PWG, is achieved in the measurement for the considered bandwidth, with typical peak-to-peak (PP) E-field amplitude and phase variations less than ±1.25 dB and ±7.5°, respectively, which demonstrated its effectiveness and robustness.

Index Terms—Plane Wave Generator (PWG), wideband dual-polarized antenna, over-the-air test, sub-6 GHz base station

I. INTRODUCTION

WITH the development of the fifth generation (5G) cellular communication in recent years, OTA test has attracted great research attention, especially for 5G sub-6 GHz BS where massive multiple-input multiple-output (MIMO) technology is largely introduced. Integrated antenna array and radio remote unit design is becoming popular. Consequently, radiated OTA testing is predicted to be inevitable for radio performance testing [1].

PWG is an efficient OTA testing method, the concept of which can be dated back to 1978 [2]. The basic principle is that a plane wave can be approximated in the proximity of the PWG array via setting suitable complex excitations for the PWG elements. To determine suitable excitations, various numerical methods have been proposed, e.g. an iterative optimization method, least square fit, genetic algorithm, and intersection algorithm [3]-[8]. A systematic study on the PWG design was

given in [9], where guidelines on size and shape of the PWG design and the number of required PWG elements were discussed. The PWG design has been, however, mainly investigated in theoretic analysis, clearly lacking of practical applications. Only in recent years, several commercial PWG designs were reported [10], [11], [12], though its design details were not given. Furthermore, only the PWG design in [11] has truly addressed ‘wide-band’ and dual-polarized PWG design.

In typical PWG design, each PWG element is excited by a complex coefficient, which is often realized by programmable phase shifter and attenuator. A massive PWG array is expected for massive MIMO sub-6 GHz BS. Major limiting factors for PWG design include its high cost, its complicated feeding network, and support for wideband scenarios. In this paper, several novel strategies are proposed to address the above-mentioned challenges. Unlike conventional PWG design with complex excitation for each PWG element, a novel tapered amplitude-only excitation method (i.e. without the need for individual phase excitation) is proposed. The proposed method can greatly reduce the feeding network complexity and reduce mutual coupling [13] among PWG elements. Furthermore, a sub-array concept is adopted where each sub-array is excited instead of excitation for each PWG element. The sub-array concept can significantly reduce the number of excitation channels, and therefore to reduce the cost. Unlike traditional uniform design which lacks support for ultra-wideband operations, a non-uniform configuration is proposed.

II. PWG OPTIMIZATION STRATEGIES

A. Tapered amplitude-only excitation method

A new PWG element excitation method based on tapering function is discussed in this part. Based on the theory of compact range (CR) reflector, a plane wave region can be generated by uniform planar current and the edge truncation effect can be significantly reduced through the design of the CR edge tooth [14], [15]. The aperture field distribution of the CR follows the tapering function shown in (1) [14]:

$$e = [1 + (\alpha \frac{|x|}{A_x})^\beta]^\gamma [1 + (\alpha \frac{|y|}{A_y})^\beta]^\gamma \quad (1)$$

where A_x and A_y equal to half of the side length of the aperture in the x and y direction, respectively, with x and y denoting the

Yusheng Zhang, Zhengpeng Wang, Xuelei Sun, Zhaolong Qiao, and Jungang Miao are with Electromagnetic Laboratory, School of Electronic and Information Engineering, Beihang University (BUAA), Beijing, China 100191 (e-mail: zhangys10@buaa.edu.cn; wangzp@buaa.edu.cn; xlsun@buaa.edu.cn; qiaozhaolong@buaa.edu.cn; jmiaobremen@buaa.edu.cn).

Wei Fan is with the Antennas, Propagation, and Millimeter-wave Systems (APMS) Section, Department of Electronic Systems, Faculty of Engineering and Science, Aalborg University, Denmark (e-mail: wfa@es.aau.dk).

PWG element coordinates with the origin at the center of the rectangular aperture. α, β, γ are parameters to be optimized for the tapering function. Basically, we set the size and depth of the quiet zone at a specified distance to the PWG, and α, β and γ are design parameters which render optimal quiet zone field distribution performance for a specific PWG design. This distribution law has inspired us to apply the tapering function to the PWG design. Equation (1) provides the framework to determine the amplitude excitation for the PWG design, with only three parameters α, β, γ to be optimized. The near-field distribution (which is determined by the transfer function from the PWG to the quiet zone) is calculated based on the simple free-space propagation formula of a point source [8, 9, 16]. The PWG design parameters α, β, γ in (1) are frequency dependent, due to the fact that the transfer function is frequency dependent.

Compared to existing excitation methods, there are several unique advantages of our proposed method. We only need to control the amplitude excitation of the PWG elements without adjusting the phase excitation. By doing so, we can greatly simplify the feeding network design. In conventional PWG methods, we often need to optimize the amplitude and phase excitations of elements with constraints, which can be computationally prohibitive, especially for large-scale PWG design [17]. With our proposed method, only three parameters of the tapering function need to be optimized for each frequency band, which can reduce the complexity significantly.

B. Non-uniform PWG configuration

One major drawback of the PWG compared with CR is the narrow working frequency range. The main reason for the bandwidth limitation is that discrete units are employed in the PWG. The minimum spacing depends on the aperture size of the antenna elements which is determined by the lowest working frequency. It is well known that the large element spacing in the uniform array would lead to grating lobe in the far field and high electromagnetic field ripples in near field. Therefore, non-uniform arrays are used to improve the performance of the PWG at high frequencies in order to broaden the entire working bandwidth of PWG.

The 2D non-uniform configuration is designed as below. We first design a non-uniform linear array, which is composed of 16 PWG elements, with a length of 28λ at 4.9 GHz (i.e. approximately 1.7 m). The center-aligned observation line with a length of 0.9 m is set parallel to the linear PWG array at the distance of 2.1 m. The non-uniform PWG is designed with the brute-force strategy, where we first set 56 half wavelength spaced potential positions in the linear array, 16 of which will be selected eventually for the PWG elements. Due to the symmetry of the linear array and two positions fixed at two ends of the linear array, we will have in total C_{27}^M arrangements, where C_N^M is a combination operator. For each possible 16 element non-linear PWG design, we can obtain the amplitude and phase distribution of the E-field on the observation line. The optimal non-uniform arrangement, which offers the lowest amplitude and phase ripples is selected. The brute-force method, though computationally heavy, offers an effective way to find the feasible non-uniform configuration.

After obtaining the optimal non-uniform 16-element linear PWG, we extend it to a 2D 256 element non-uniform square PWG via the simple meshing operation with symmetric and

squared PWG configuration. Note that, the PWG configuration and element position are fixed for all considered frequencies, yet the amplitude excitations are re-optimized for each frequency according to (1), as explained in Section II.

C. Sub-array strategy

In principle, a PWG design with independent excitations for all elements can achieve better quiet zone performance, compared to the PWG design with independent excitation for each sub-array. However, a large-scale PWG is prohibitively expensive and challenging to implement in practice. Therefore, the sub-array strategy is adopted as an alternative to reduce the number of excitation channels. The objective is that we would like to minimize the number of excitation channels while still maintaining similar quality of the quiet zone performance. The sub-array design strategy is explained below.

From (1), the amplitude excitations of 256 elements in the non-uniform PWG array can be obtained once the PWG configuration is known. With the sub-array concept, we only have 64 feeds, since each subarray is composed of 4 PWG elements, as shown in Fig. 2. We have homogenous amplitude and phase excitation for the four elements in the sub-array. The amplitude excitation for each sub-array is the average of amplitude excitations of its four associated sub-array PWG elements. In our design, only the amplitude excitations for the 64 feeds should be obtained, since the phase excitations are the same for all 64 sub-arrays. Note that the obtained amplitude excitations for the 64 sub-arrays will be used as initial values to be used in a genetic algorithm (GA) to obtain the final amplitude excitations for the 64 sub-arrays [5].

III. 16×16 PWG DESIGN

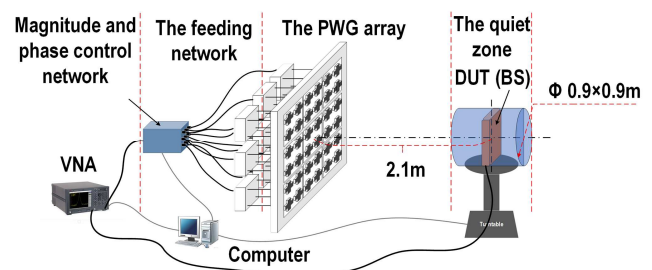


Fig. 1. The PWG system configuration.

The proposed PWG design consists of three main parts, as shown in Fig. 1, the 16×16 non-uniform planar antenna array, the feeding network, and the amplitude and phase control network. The 1.7m × 1.7m, 256 elements square PWG array is the core part of the system. Appropriate absorbing materials are installed in the array to reduce element mutual coupling and multiple reflection effects. Quad-ridged waveguide antenna is employed as the PWG element, since it is dual polarized, covers 2 to 6 GHz, offers homogenous antenna pattern, good consistency, good port isolation (higher than 25 dB) and excellent polarization isolation (more than 50 dB at 3.5 GHz). The geometry of the antenna element is shown in Fig. 2. Note that a 72 mm square waveguide is used as a shell for the antenna element to reduce cost and improve homogeneity between the

elements. The initial location of the quiet zone is set to 1.5 times of the PWG array aperture, which comes from the design experience in CR. During the design, we aim to reduce the distance between the PWG aperture and the quiet zone based on numerical optimization. However, too small measurement distance would lead to coupling between the PWG and DUT. The final quiet zone design (i.e. a cylinder quiet zone of 0.9 m diameter and 0.9 m depth, with a measurement distance of 2.1 m) is a compromise of these factors. Note that the same physical quiet zone at different frequency band is aimed, which is convenient for practical applications.

An amplitude and phase control network with 32/64 ports is relatively popular, and a 1 to 4 equal power divider is a mature product and suitable for massive production. Therefore, a 16×16 PWG design is implemented with 64 4-element sub-arrays in our study. Four neighboring PWG elements are grouped in a sub-array, where three different sub-array configurations exist, i.e. 2×2, 4×1 and 1×4, as illustrated in Fig. 2 (left). The PWG elements are grouped into sub-arrays based on two basic principles. First, close-by elements in geometry should be grouped together to reduce the complexity of the feeding network. The second one is that elements with similar excitations are grouped to form a sub-array to reduce the effect of feeding difference on the quiet zone performance. Therefore, it is an optimal solution given the trade-off between quiet zone performance and easy assembling and wiring in practice.

The four elements in the sub-array are combined (with equal phase and amplitude excitation within each sub-array) with the help of the 1 to 4 equal power divider, and each sub-array is independently excited with weights determined by the tapered amplitude-only method explained earlier. Each element retains its original position when forming sub-arrays. The final design of the PWG sub-array arrangement is shown in Fig. 2. Note that dedicate arrangement of the sub-arrays is required to reduce the quiet zone quality deterioration introduced by discontinuity of the feeding distribution. Even so, additional excitation magnitude optimizations are required. A 1 to 4 power divider, a high-reliability relay switch, and 11 coaxial cables are used to feed each sub-array, as shown in Fig. 2. Two sets of power divider network and one set of switch network are used to achieve dual polarized feeding requirements, as shown in Fig. 2. 64 RF switches are employed to switch the polarization of the PWG. All the switches are connected to an amplitude-phase control network which is used to configure the designed amplitude and phase distribution of the array.

In our work, the amplitude taper is achieved by the amplitude and phase control network. Each sub-array is fed by an RF path from the network composed of programmable attenuator (60 dB dynamic range, 0.25 dB step) and phase shifter (360° range with 8 bits). The amplitude and phase control network is used 1) to calibrate out the inhomogeneities among RF paths connected to the PWG sub-arrays, and 2) to implement the amplitude taper for each considered frequencies. However, the requirements for the desired phase adjustment range are very low. Note that the amplitude taper can be achieved by accurately controlling the amplitude excitation in the fixed attenuator in principle. However, this requires that we have

homogenous RF chains in design. Also, another difficulty is to implement amplitude tapers for several frequencies if the amplitude control is fixed.

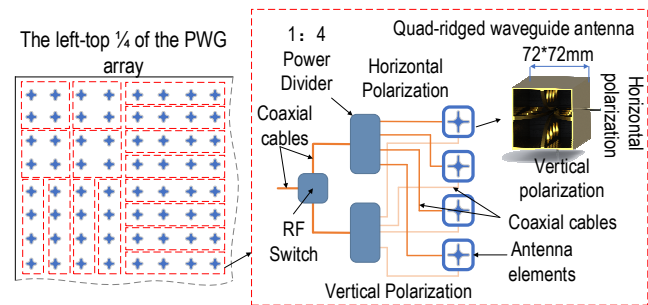


Fig. 2. The layout of the upper-left 1/4 PWG (left) and Quad-ridged waveguide antenna and subarray (right).

The final designed PWG element configuration and amplitude excitations are shown in Table I. In the non-uniform PWG configuration, we give the coordinates of each antenna element as follows: $(x_1, x_2, \dots, x_8) = (-0.8025\text{m}, -0.7035\text{m}, -0.601\text{m}, -0.4915\text{m}, -0.3805\text{m}, -0.2745\text{m}, -0.16\text{m}, -0.0595\text{m}) = (y_1, y_2, \dots, y_8)$. As explained, the 256 PWG element locations can be obtained through combining the X and Y coordinates with meshing operation and array geometry symmetry. Note that only the feeding amplitude of the sub-arrays on the upper-left 1/4 part of the PWG are listed, and the rest can be obtained based on axis symmetry.

TABLE I
THE FEEDING WEIGHTS OF THE UPPER-LEFT 1/4 PART OF THE PWG

Feeding Weights(dB)	Element index in X direction							
	1	2	3	4	5	6	7	8
2.6/3.5/4.9GHz	16	-26/-26/-60	-10.5/-9.1/-20			-8/-10.5/-14		
	15					-8/-5.2/-6		
Element index in Y direction	14	-10.5/-9.1/-20	-3.1/-3.7-5.2			-0.9/-1.9/-1.9		
	13					-2.5/-0.4/-0.4		
	12					0/0/0		
	11	-8/-10.5/-14	-0.9/-1.9-1.9			0/0/0		
	10					0/0/0		
	9	-8/-10.5/-14	-0.9/-1.9-1.9			0/0/0		

IV. NUMERICAL SIMULATIONS AND EXPERIMENTAL VALIDATIONS

In this section, the simulation and measurement results of the designed PWG system covering sub-6GHz bands are illustrated.

A. Simulation results

The designed PWG is simulated in the CST software. Three sets of feeding weight of the array elements are optimized at center frequency 2.6 GHz, 3.5 GHz and 4.9 GHz, respectively, to cover the whole operating band, applying tapered amplitude-only excitation method. The cylindrical quiet zone is achieved, with a peak-to-peak amplitude and phase deviation of ±0.8 dB and ±7°, respectively. The simulation results at the central section of the quiet zone (i.e. at 2.1m) at 2.6 GHz, 3.5 GHz and 4.9 GHz are shown in Fig. 3. It can be observed that the designed PWG supports ultra-wideband operation with good accuracy. The quiet zone performance is also well maintained

over 0.9 m depth, where peak-to-peak magnitude and phase deviation up to ± 0.9 dB and $\pm 6^\circ$ can be obtained for distance 1.65 m, 2.1 m and 2.55 m at 3.5GHz. Furthermore, a polarization purity of more than 30 dB within the quiet zone at 3.5 GHz is achieved in simulation, indicating an excellent polarization purity within the quiet zone.

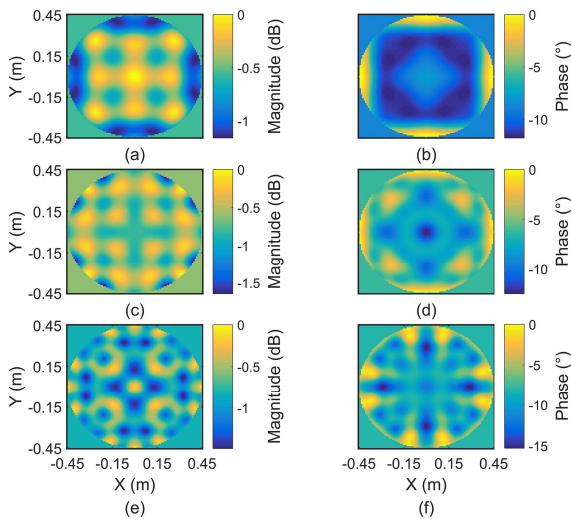


Fig. 3. The simulation E_y of the quiet zone of 2.1m at 2.6 GHz (a, b), 3.5 GHz (c, d) and 4.9 GHz (e, f). Note that the amplitude and phase outside the quiet zone are averaged. This applies for Fig. 5 as well.

B. Measurement results

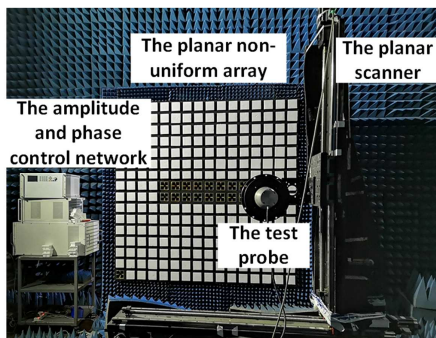


Fig. 4. Photo of the system and the test setup.

The designed PWG was experimentally validated in the anechoic chamber. Fig. 4 shows the prototype of the system and the test setup. The white square in front of the antenna is a radome, which consists of the foam material with a dielectric constant close to 1. A planar scanning system is applied to record the field distribution in quiet zone section at the distance of 2.1m from the PWG array interface. The vertically polarized E-field distribution of the quiet zone is measured at three typical operation frequencies, 2.6 GHz, 3.5 GHz and 4.9 GHz. The magnitude and phase deviation at each frequency is less than ± 1 dB and $\pm 9^\circ$, respectively, as shown in Fig. 5.

Fig. 6 presents the measured PP magnitude and phase deviation comparisons in the whole quiet zone field at typical sub-6 GHz frequencies. The PP deviations for both the

simulation and the test results in Fig. 6 are obtained by evaluating the difference between the maximum and minimum values of the amplitude and phase of the electric field at all sampling points. The results demonstrate quite good quiet zone quality and ultra-wideband characteristics of the PWG system. The minor deviations compared with simulation results are introduced by mutual coupling and feeding signal magnitude and phase uncertainties. Even though there are many non-ideal factors in the measurement system, the system still shows good stability and achieves good quiet zone performance, which indicates the effectiveness and robustness of our PWG design.

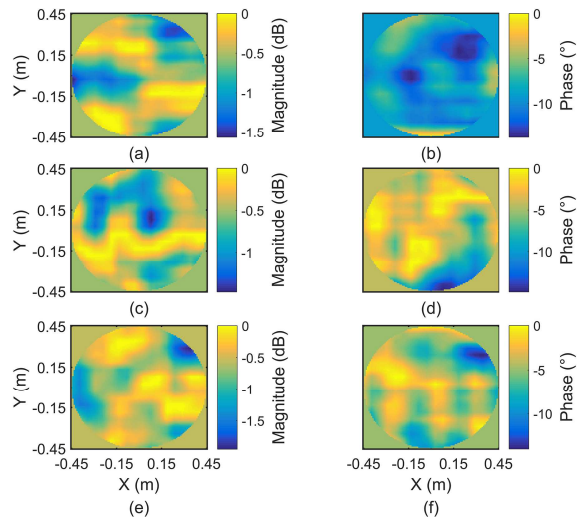


Fig. 5. The 2-D measured E_y of the quiet zone of 2.1m at 2.6 GHz (a, b), 3.5 GHz (c, d) and 4.9 GHz (e, f).

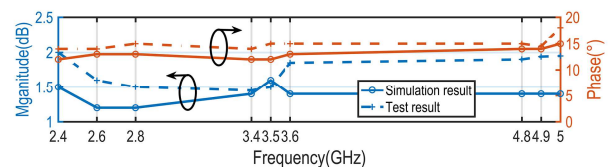


Fig. 6. The whole quiet zone deviation comparisons of the simulation results and measured results at typical sub-6 GHz frequencies.

V. CONCLUSION

A novel 16×16 dual-polarized plane wave generator (PWG) design is proposed for 5G BS OTA test in the paper. Three strategies are proposed and implemented in the proposed PWG: tapered amplitude-only excitation method to reduce feeding network complexity and mutual coupling among PWG elements; non-uniform PWG configuration to support for ultra-wideband operations; and sub-array design (with power splitter) to reduce required number of excitation channels. The proposed PWG is highly robust, simple and cost-efficient. The designed PWG is numerically simulated and experimentally validated. A plane wave quiet zone with the typical PP E-field amplitude and phase variation up to ± 1.25 dB and $\pm 7.5^\circ$ respectively is achieved in the measured results for frequencies ranging from 2.4 GHz to 5 GHz. The proposed PWG design will be of high value for 5G sub-6 GHz BS OTA testing.

REFERENCES

- [1] R. Xie et al., "Synthesis of plane wave applied to 5G communication antenna measurement," 2017 Progress In Electromagnetics Research Symposium - Spring (PIERS), St. Petersburg, 2017, pp. 195-198, doi: 10.1109/PIERS.2017.8261732.
- [2] J. C. Bennett and E. P. Schoessow, "Antenna near-field/far-field transformation using a plane-wave-synthesis technique," in Proceedings of the Institution of Electrical Engineers, vol. 125, no. 3, pp. 179-184, March 1978.
- [3] G. T. Poulton, "An alternative plane wave synthesis method for Fresnel-zone antenna measurements," Digest on Antennas and Propagation Society International Symposium, San Jose, CA, USA, vol.1, pp. 90-93, 1989.
- [4] D. F. Groutage, J. D. Gary and D. K. Owen, "Near-field plane wave generation using a minimum mean square error approach," [1992] IEEE Sixth SP Workshop on Statistical Signal and Array Processing, Victoria, BC, Canada, 1992, pp. 516-521, doi: 10.1109/SSAP.1992.246896.
- [5] Ding Yu, Ning Zhang and Ping Xu, "Synthesis of a plane wave in the near field using genetic algorithm," Proceedings of the 9th International Symposium on Antennas, Propagation and EM Theory, Guangzhou, pp. 810-813, 2010.
- [6] H. Wang, J. Miao, J. Jiang, R. Wang and Z. Lei, "Generating plane waves in the near fields of pyramidal horn arrays," ISAPE2012, Xian, pp. 211-218, 2012.
- [7] Á. F. Vaquero, D. R. Prado, M. Arrebola, M. R. Pino and F. Las-Heras, "Near field synthesis of reflectarrays using intersection approach," 2017 11th European Conference on Antennas and Propagation (EUCAP), Paris, pp. 3644-3648, 2017.
- [8] M. D'Urso, G. Prisco and M. Cicolani, "Synthesis of Plane-Wave Generators via Nonredundant Sparse Arrays," in IEEE Antennas and Wireless Propagation Letters, vol. 8, pp. 449-452, 2009.
- [9] O. M. Bucci, M. D. Migliore, G. Panariello and D. Pinchera, "Plane-Wave Generators: Design Guidelines, Achievable Performances and Effective Synthesis," in IEEE Transactions on Antennas and Propagation, vol. 61, no. 4, pp. 2005-2018, April 2013.
- [10] R&S Report (2019). Report on R&S@PWC200 Plane Wave Converter For 5G massive MIMO base station testing, March, 2019. Rohde & Schwarz USA, Inc. https://scdn.rohde-schwarz.com/ur/pws/dl_downloads/dl_common_library/dl_brochures_and_datasheets/pdf_1/PWC200_fly_en_5215-5971-32_v0200.pdf.
- [11] F. Scattone et al., "Design of Dual Polarised Wide Band Plane Wave Generator for Direct Far-Field Testing," 2019 13th European Conference on Antennas and Propagation (EuCAP), Krakow, Poland, 2019, pp. 1-4.
- [12] S. Sun, N. Wang, X. Ma, S. Zhu and R. Wang, "Design of Plane Wave Generator in Compact Range for 5G OTA Testing," 2019 Photonics & Electromagnetics Research Symposium - Fall (PIERS - Fall), Xiamen, China, pp. 1011-1014, 2019.
- [13] X. Chen, S. Zhang, and Q. Li, "A review of mutual coupling in MIMO systems," IEEE Access, vol. 6, pp. 24706 - 24719, 2018.
- [14] Guoyu He. Calculation and measurement of electromagnetic scattering. Beijing, China: Beihang University Press, 2006.
- [15] Quan S., Studies on Compact Range Design, Evaluation and Applications. 2003, in Chinese.
- [16] J. C. Hong, H. Fang, X. Z. Jiang and G. Y. He, "Convolution method of Antenna Near Field Calculation[J]. Acta Electronic Sinica, pp. 112-114, September 1997.
- [17] X. Sun, Z. Wang and J. Miao, "Near Field Quasi Plane Wave Generation and Performance Evaluation," 2018 Asia-Pacific Microwave Conference (APMC), Kyoto, 2018, pp. 917-919, doi: 10.23919/APMC.2018.8617156.